Thermo-electromechanical responses of 1-butyl-3-methylimidazolium chloride ionic liquid-cellulose gel

2 **AUTHORS**, INCLUDING:

Anuvat Sirivat

Chulalongkorn University

232 PUBLICATIONS   **2,220** CITATIONS

ORIGINAL PAPER

Thermo-electromechanical responses of 1-butyl-3-methylimidazolium chloride ionic liquid-cellulose gel

Wissawin Kunchornsup · Anuvat Sirivat

Abstract 1-butyl-3-methylimidazolium chloride (BMIM$^+$Cl$^-$) is an ionic liquid utilized as an effective cellulose gelling agent for the fabrication of BMIM$^+$Cl$^-$ cellulose gel, called CelGel. The little-known transient thermo-electromechanical responses are investigated via an oscillatory shear experiment, under absence and presence of an electric field at equilibrium and non-equilibrium between 30 ˚C and 60 ˚C. In the equilibrium state with no electric field, the shear storage modulus (G′) increases with increasing temperature due to the stronger interaction between the cellulosic hydroxyl group and the chloride anion. In the equilibrium state with an electric field of strength 1 kV/mm , G′ continuously decreases with increasing temperature as chloride anions move out of crosslinking positions to become polarized under the electric field. The heating rate effect in the absence of an electric field is investigated between 0.5 and 20.0 °C/min. In the temperature-increasing step, G′ significantly increases because of the stronger interaction, along with cellulose chain expansion. In the temperature-decreasing step, G′ remains at its higher value, as it needs a longer time to relax. The heating rate effect in the presence of an electric field is also investigated. In the temperature-increasing step, G′ increases with a slower rate because of a shorter time scale required for the BMIM$^+$ polarization. In the temperature-decreasing step, a recrystallization occurs at a lower temperature because the shorter time scale obstructs the recrystallization process. Thus, transient thermo-electromechanical properties of CelGel have been systematically investigated here for the first time under the thermal equilibrium and non-equilibrium states.

Introduction

Cellulose consists of β-(1→4)-linked glucose repeating units [1].The non-centrosymmetry refers to its internal rotation of polar atomic groups associated with asymmetric carbon atoms which contribute to the piezoelectric properties of cellulose [2]. However, the strong inter-molecular and intra-molecular hydrogen bondings of the cellulosic hydroxyl group in the dissolution process are well known to be the main obstacle in utilizing cellulose. Kim and coworkers investigated cellulose as a smart material, termed electroactive paper (EAPap), via the xanthate reaction system in 2006. They prepared films which demonstrated drastic actuation performances based on two actuation mechanisms: the dipolar orientation of the hydroxyl group of cellulose and the water-bound Na$^+$ cation motion [3]. In addition, EAPap is ultra-lightweight, inexpensive, and biodegradable.

Some of the well-known cellulose solvents are the ionic liquids or the ionic compounds which exist as liquids at low temperature [4, 5]. Their interesting properties are high stability, suitable polarity, high ionic conductivity, and easy recyclability [6]. Nafion™ swollen in 1-ethyl-3-methylimidazolium bis(triflouromethyl- sulfonyl)imide (EMI-IM) has been studied by Bennett and coworkers in 2006 [7]. They showed that the actuation speed and the ionic conductivity could be increased by increasing counterion size and increasing content of the ionic liquid, with the counterions acting as the primary charge carriers [7]. The use of EMI-IM was then demonstrated as a solvent for Nafion™ polymer actuators and sensors. The Nafion™ polymer actuators solvated with this ionic liquid possessed improved stability when

W. Kunchornsup · A. Sirivat (✉)
The Petroleum and Petrochemical College,
Chulalongkorn University, Bangkok 10330, Thailand
e-mail: anuvat.s@chula.ac.th

operated in air in comparison to the same materials solvated with water [8].

1-Butyl-3-methylimidazolium chloride (BMIM$^+$Cl$^-$), a well-known ionic liquid, was utilized in the previous work as the gelling agent for a microcrystalline cellulose [9–11], named CelGel. Kadokawa et al. [2008] reported a dissolution of 13 % cellulose via 87 % BMIM$^+$Cl$^-$ at 100 °C [9]. Furthermore, N, N-dimethylacetamide (DMAc) was added as a physical gelling agent to plasticize the viscous solution [10, 11]. The electromechanical properties of the cellulose gels were investigated under the oscillatory shear mode at electric field strengths between 0 and 1 kV/mm, and as functions of temperature. The shear storage modulus (G′) increased linearly with temperature up to 60 ˚C at 1 rad/s in the absence of an electric field. G′ also increased linearly with temperature up to 40 ˚C at 1 rad/s in the presence of 1 kV/mm of electric field strength and decreased above 40 ˚C, consistent with the behavior of dielectric permittivity (ε′). In the deflection experiments under an applied DC electric field, the deflection distances of the gels linearly increased with increasing electric field strength along with the dielectrophoresis forces above the electrical yield strength of 100 V/mm [10, 11]. In addition, it was known that temperature in an actuator system can be increased via a heat build-up process under high electrical frequency, electric field strength, and strain amplitude [12–14]. The temperature factor has been of remarkably concern for materials used in actuator applications.

Putz and Burghelea [2009] studied the temperature effect between 5 ˚C and 20 ˚C on solid–fluid transition of Carbopol® 940, or sodium polyacrylate, in the polyanion family [15]. The solid–fluid transition in terms of dynamic elastic modulus was strongly influenced by temperature through competition between destruction and reformation of the gel. A microscopic scale scenario for the competition between break-up and recombination of solid structure elements and the mediating role of temperature was explained in two regimes. In the low temperature regime, free polymer chains explored a limited number of possible configurations because of weak Brownian motion. Thus, the probability for different chains to come into an effective binding range was small, and over long enough periods of time, the shear-induced destruction of soft structural units dominated. An increase in temperature reversed the effect. The Brownian motion of free polymer chains was strong enough to bring free molecules into an interacting range; thus, the recombination of the network became probabilistically plausible [15]. Ruan and coworkers [2008] studied different gelling behaviors of cellulose solution dissolved in aqueous NaOH/thiourea between −5 ˚C and 40 ˚C [16]. The time dependence of G′ and G″ for 5 wt% cellulose solution under different temperatures at ω=1 rad/s was investigated. The solution was able to remain as a viscous liquid at 0 ˚C without gelling. Interestingly, the gelation of the cellulose solution took place easily at 30 ˚C. It was suggested that the

rheological properties of the cellulose solution were strongly sensitive to temperature. In the cellulose solution system, the inclusion complex (IC) structure was formed through hydrogen-bonding networks. With an increase in temperature, the hydrogen-bonding network structure of IC could be destroyed and self-associated to form a gel. However, the IC became less stable and produced a lower equilibrium modulus when gelation temperature increased [16]. The temperature could also influence electrical conductivity of poly(tetrahydrofuran) when the tetrahydrofuran-repeating unit was partially decomposed upon thermal cycling, resulting in a self-plasticizing effect [17]. This suggested a novel processing strategy that could combine the conductivity performance of gel with the processing advantage of polymers. Moreover, the decomposed tetrahydrofuran was further susceptible to the formation of explosive peroxides that were likely to have limited application [17].

Li and coworkers [2007] studied temperature effect on the high amplitude vibration of piezoelectric bending actuators [14]. Temperature was increased with increasing frequency, electric field, and vibration amplitude due to higher mechanical and electrical losses. The uneven stress distribution had resulted in a high-to-low gradient temperature rise from the clamped end to the free end of the actuator [14]. Time-temperature profiles of multi-layer soft lead zirconate titanate actuators were investigated by Pritchard and coworkers [2004] [12]. The investigation of temperature rise of actuators as a function of operation conditions (frequency, electric field magnitude and polarity, actuator mounting, and material properties) was important in accelerated lifetime testing of these devices. The temperature rise was found to be approximately proportional to the frequency, while the total loss of the actuator per cycle increased with applied field and frequency. The rise of temperature can lead to overheating, thermal degradation, depolarization, and electrode delamination due to loss mechanisms contributing to heat generation [12]. Yoon [2012] studied the effect of temperature on the actuation performance of electro-fluid-thermal-compliant (ETC.) actuators [13]. The electric potential caused built-up temperature in the actuator and produced more actuation displacement. When rising heat was dissipated via surrounding media with high thermal and electrical conductivities, actuation displacement was decreased [13].

Both cellulose and ionic liquids are interesting for use as electroactive materials due to the piezoelectric [3] and ionic polarizations [11], respectively. The cellulose is used for polarizable scaffolding to trap ionic liquid and exhibits mixed electronic-ionic polarization effects for electroactive applications. Both materials could be mixed and fabricated by sol–gel processes [10]. In the present work, we are interested in investigating the transient thermo-electromechanical responses of BMIM$^+$Cl$^-$cellulose gel, named CelGel, via oscillatory shear experiment. The thermo-electromechanical

responses under absence and presence of an electric field at equilibrium and non-equilibrium are reported here. In addition, thermo-chemical properties at equilibrium and thermal properties at non-equilibrium under absence of an electric field are investigated via Fourier transform infrared spectroscopy (FTIR) and differential scanning calorimetric (DSC), and shall be reported here.

Experimental

Materials

Cellulose microcrystalline powder (AR grade, Sigma-Aldrich), 1-butyl-3-methylimidazolium chloride (BMIM$^+$Cl$^-$) (HPLC grade, Sigma-Aldrich), and N,Ndimethylacetamide (DMAc) were used as received without further purification.

Preparation of 1-butyl-3-methylimidazolium chloride ionic liquid-cellulose gel (CelGel)

BMIM$^+$Cl$^-$ and the dried cellulose were mixed at a composition of 87 % w/w of BMIM$^+$Cl$^-$ (2.15 g) and 13 % w/w of cellulose (0.323 g) , equivalent to a 6.19:1 molar ratio of BMIM$^+$Cl$^-$: glucose [9], as this molar ratio allows the maximum dissolution of cellulose in BMIM$^+$Cl$^-$ at 100 °C. The cellulose was dissolved in BMIM$^+$Cl$^-$ at 100 °C for 15 minutes. The obtained viscous solution was filled with 1.5 ml of N, N-dimethylacetamide (DMAc) as a plasticizer and a co-solvent, and was stirred for 60 minutes. The solution was degassed and cast into a mold having a diameter of 25 mm and a thickness of 1 mm, and kept under a vacuum for 12 hours. The 1-butyl-3-methylimidazolium chloride ionic liquid-cellulose gel (CelGel) was obtained after curing at ambient conditions for 24 hours [10]. The CelGel was then characterized for thermo-electromechanical responses under absence and presence of an electric field.

Characterization of prepared CelGel

To investigate the chemical structure of the CelGel at different temperatures, FTIR was used (Thermo Nicolet, Nexus 670), using a ZnSe (zinc selenide) crystal, a resolution of 4.0 cm^{-1}, a scan number of 64, and a wavenumber range of 750–4000 cm^{-1}. The CelGel was pasted on the ZnSe and measured with increasing and decreasing temperature between 30 °C and 60 °C.

To investigate the thermal properties of the CelGel at different heating rates, the differential scanning calorimetric (DSC) curve was measured under N$_2$ atmosphere, corresponding with a programmed temperature profile via a simultaneous thermal analyzer (STA), Netzch STA 449 F3. The procedure of temperature programming was: holding at 30 °C for 5 min;

increasing from 30 °C to 60 °C with a certain heating rate; holding at 60 °C for 5 min; decreasing from 60 °C to 30 °C with a certain heating rate; and holding at 30 °C for 15 min.

The thermo-electromechanical properties were measured by a rheometer (Rheometric Scientific, ARES) fitted with a parallel plate fixture (diameter 25 mm). DC voltage was applied with a DC power supply (Instek, GFG 8216A), which can deliver an electric field up to 4 kV. A digital multimeter (Tektronix, CDM 250) was used to monitor the voltage input. The samples were prepared in the configuration of a Polyimide/CelGel/Polyimide sandwich to prevent the shortening of the circuit. The Polyimide (PI), ®Kapton TH-012 (12 micron) was produced by and obtained from ©2006 Saint Gobain Performance Plastic Corporation. The PI film represents an excellent insulator up to 7 kV/mm for preventing a voltage breakdown; with a dielectric constant value of 3.3, and a volume resistivity >10 ^{16}Ω-cm. In these experiments, an oscillatory shear strain was applied. Strain sweep tests were first carried out to determine the suitable strains to measure G′ in the linear viscoelastic regime[11]. The appropriate strain was determined to be 0.25 % for the CelGel study. To determine relaxation time (τ_r) at 60 °C under absence and presence of an electric field, the stress relaxation (G′(t) vs t) of CelGel was measured. It was transformed to the relaxation spectrum (H(λ) vs λ) and the storage moduli crossover (G′ and G″ vs frequency). τ_r, the relaxation time, was determined as the reciprocal of the crossover frequency [18]. The thermo-electromechanical response at equilibrium was investigated in the time sweep test mode between 30 °C and 60 °C with 100 rad/s and 0.25 % strain under absence and presence of an electric field. The steady G′ of certain temperature and electric field strength was plotted in terms of G′ vs. temperature. The thermo-electromechanical response at non-equilibrium was investigated in the mode of temperature sweep test mode with 100 rad/s and 0.25 % strain. The procedure for the temperature sweep test is: holding at 30 °C for 5 min; increasing from 30 °C to 60 °C with a certain heating rate (0.5 or 20.0 °C/min); holding at 60 °C for 5 min; decreasing from 60 °C to 30 °C with a certain heating rate; and holding at 30 °C for 15 min, respectively.

As shown in Table 1, the criteria for non-equilibrium is $\tau_m \ll \tau_e \ll \tau_r$; they are the measuring, experimental, and relaxation time scales, respectively. The measuring time scale (τ_m) refers to the reciprocal of ω of the measured G′(ω), which is 10^{-2} s at ω=100 rad/s of frequency. The experimental time scale (τ_e) was ∞, 120, and 3 s, corresponding to 0, 0.5, and 20.0 °C/min of heating rates, respectively. The relaxation time scale (τ_r) was determined from the reciprocal of the crossover frequency at 60 °C, which is 2.84×10^3 s and 2.75×10^3 s at the electric field strengths of 0 and 1 kV/mm, respectively. The data suggeststhat the cellulose chain in CelGel dominates the relaxation behavior in all conditions with a long time scale. The criteria for equilibrium is $\tau_m \ll \tau_e \gg \tau_r$, in which τ_e is

Table 1 Measuring time scale (τ_m), experimental time scale (τ_e), and relaxation time scale (τ_r) of CelGel at different electric field strengths and heating rates

Electric field strength (kV/mm)	Heating rate (°C/min)	τ_m (s)	Comparison	τ_e (s)	Comparison	τ_r (s)	State
0	0.0	10^{-2}	<<	∞	>>	2.84E+03	equilibrium
	0.5	10^{-2}	<<	120	<<	2.84E+03	non-equilibrium
	20.0	10^{-2}	<<	3	<<	2.84E+03	non-equilibrium
1.0	0.0	10^{-2}	<<	∞	>>	2.75E+03	equilibrium
	0.5	10^{-2}	<<	120	<<	2.75E+03	non-equilibrium
	20.0	10^{-2}	<<	3	<<	2.75E+03	non-equilibrium

Note: The τ_m is determined by the reciprocal of 100 rad/s, which is equal to 10^{-2} s. The τ_e is determined by reciprocal of the certain heating rate. The τ_r is determined by the reciprocal of dynamic crossover frequency, $G'(\omega)=G'(\omega)$ at 60 °C, which is transformed from stress relaxation ($G'(t)$ vs t) and relaxation spectrum ($H(\lambda)$ vs λ), respectively.

infinitely large as the condition of 0 °C/min is obtained via the time sweep test. In short, the three time scales determine whether the experiment is in equilibrium or non-equilibrium. If the relaxation process has a shorter relaxation time scale compared to τ_m and τ_e, the equilibrium condition is satisfied. On the other hand, non-equilibrium is satisfied when the relaxation process timescale is longer than τ_m and τ_e.

Results and discussion

Thermo-electromechanical responses in the absence and presence of electric field at equilibrium

Figure 1 shows the thermo-electromechanical responses in the absence of an electric field at equilibrium. The shear storage modulus (G′) at 100 rad/s increases from 1.9×10^5 to 3.3×10^5 Pa with continuously increasing temperature from 30 °C to 50 °C. This is due to the fact that an increase in temperature promotes a stronger interaction between the cellulosic

Fig. 1 Shear storage modulus (G′) at 100 rad/s vs. temperature of CelGel at 0 °C/min under 0.0 kV/mm

hydroxyl group and the ionic liquid chloride anion, as evidenced from the FTIR spectra, with a lower absorbance peak at 3402 cm^{-1}[19]. However, G′ decreases to 2.9×10^5 Pa when temperature is further increased to 60 °C; this is because temperature approaches the melting temperature of BMIM$^+$Cl$^-$ (60 °C) [20] where the OH-OH cellulose interaction diminishes and induces a lower G′ [21]. In other words, a stronger cellulosic hydroxyl group-chloride anion interaction dominates from 30 °C to 50 °C and the melting process of BMIM$^+$Cl$^-$ dominates from 50 °C to 60 °C, as confirmed by the absorbance depletion of 3094 cm^{-1}. In decreasing temperatures from 60 °C to 30 °C, the thermo-electromechanical response in the absence of an electric field exhibits nearly the same values relative to the increasing temperature path due to being in the equilibrium state. Figure 2 shows the thermo-electromechanical response in the presence of 1 kV/mm electric field strength. G′ with 1 kV/mm of electric field strength is 3.0×10^5 Pa, which is higher than 1.9×10^5 Pa of the G′ in the absence of an electric field at 30 °C. This is because an electric field induces dipole moments via the ionic and electronic polarizations within the CelGel, which produce an enhanced shear storage modulus [11]. Moreover, the shear storage modulus (G′) is diminished with increasing temperature from 30 °C to 60 °C. Under the 1.0 kV/mm electric field strength, the chloride anion, acting as a crosslinking agent, leaves out of its crosslinking position and approaches the anode electrode (higher potential electrode), producing a lower G′. For the temperature path from 60 °C to 30 °C, the thermo-electromechanical responses under the presence of 1 kV/mm electric field strength exhibit nearly the same values relative to those of the increasing temperature path due to the fact that it is in the equilibrium state.
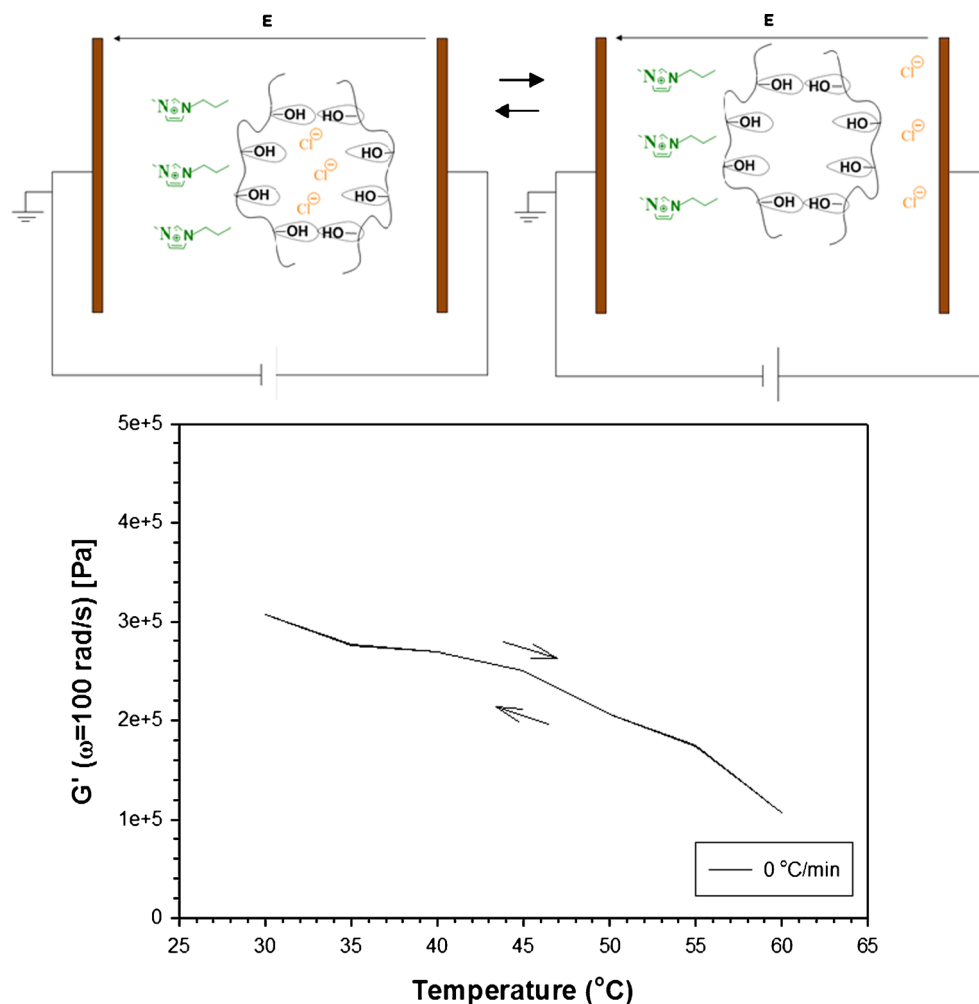
Thermo-chemical characterization at equilibrium

Figure 3 reveals the chemical interactions within and the characteristics of CelGel when temperature increases from 30 °C to 60 °C and then decreases from 60 °C to 30 °C. The
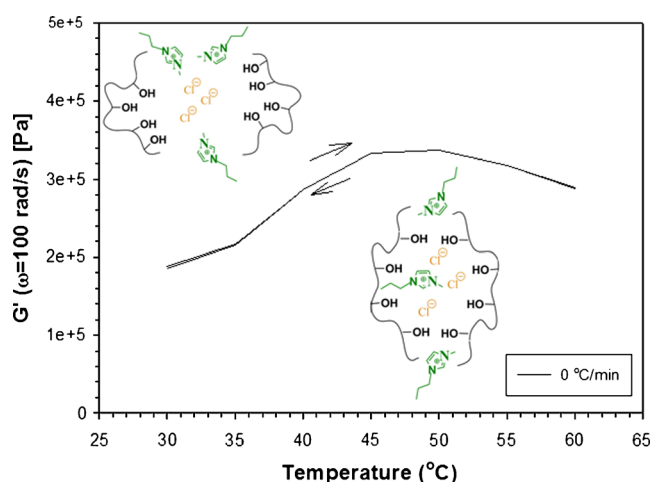
Fig. 2 Shear storage modulus (G′) at 100 rad/s vs. temperature of CelGel at 0 °C/min under 1.0 kV/mm

assignments of all FTIR interactions and characteristics are tabulated in Table 2 [19, 22–27]. The 3402 cm^{-1} absorbance peak is reduced as temperature is increased from 30 °C to 60 °C. This implies a stronger interaction between the cellulosic hydroxyl group and the chloride anion [19, 26]. In other words, a temperature increment produces a stronger crosslinking interaction and a higher G′. In addition, the 3402 cm^{-1} peak shows a stronger absorbance peak and a lower crosslinking interaction when temperature is decreased from 60 °C to 30 °C. This suggests that CelGel exhibits a reversible

Fig. 3 Fourier transform infrared (FTIR) spectra in the range of 4000 to 650 of wavenumber of CelGel between 30 and 60 °C; i=increasing step, d=decreasing step
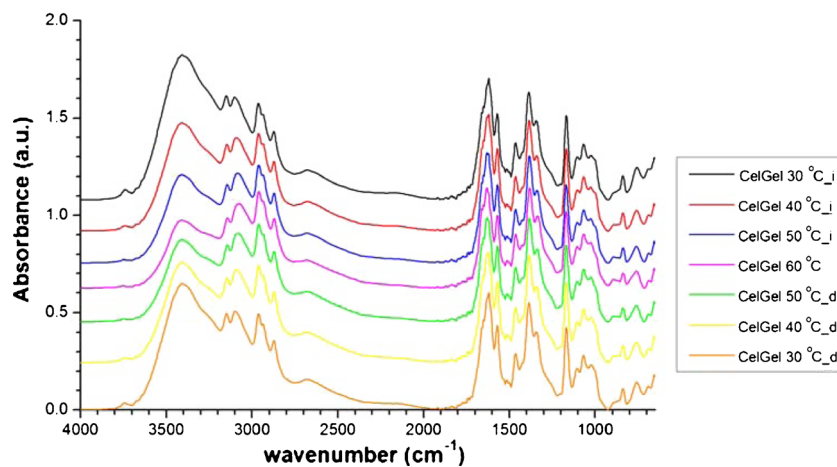
Table 2 FT-IR absorption spectrum of CelGel [19, 22–27]

| Wavenumbers (cm^{-1})	Assignments	References
1430	CH$_2$ scissoring of cellulose	[22]
897	C-O-C stretching at β-(1→4)-glycosidic linkage of cellulose	
1160	Anti-symmetric bridge stretching of C-O-C groups of cellulose	[23, 24]
1318	CH$_2$ wagging vibration of cellulose	[25]
1635-1640	Absorbed water bending vibration of cellulose	
3402	Interaction between cellulosic hydroxyl group and chloride anion	[19, 26]
2876, 2940, and 2964	C-H stretching modes of the methyl and butyl groups of BMIM$^+$Cl$^-$	[27]
3094	Coupled imidazolium C-H stretching vibrations of BMIM$^+$Cl$^-$	

thermo-stiffening effect within the temperature range of 30 °C to 50 °C. Moreover, the reversible thermo-stiffening effect does not exist when the temperature is close to 60 °C, the melting temperature of BMIM$^+$Cl$^-$ [20].

Thermo-electromechanical responses in the absence and presence of electric field at non-equilibrium

Figure 4 shows the thermo-electromechanical response in the absence of an electric field at 0.5 °C/min. In the increment step from 30 °C to 60 °C, G′ increases from 1.7×10^5 to 3.1×10^5 Pa because of a stronger cellulosic hydroxyl group and chloride anion interaction [19]. In the holding step at 60 °C and the temperature-decreasing step from 60 °C to 43 °C, G′ is higher than that of the increasing step. This is due to the strong residual crosslinking interaction. However, from 43 °C to 30 °C in the decreasing step, G′ is lower than that of the increasing step because a recrystallization of BMIM$^+$Cl$^-$ gradually occurs during the cooling, as confirmed by DSC curves. The ionic liquid molecules may reorder to crystallize themselves to produce lesser chloride anion crosslinking species, and thus a lower G′. In the holding step at 30 °C, G′ increases to obtain nearly the same initial G′, as CelGel needs a certain

time period for molecular rearrangement, thus providing a reversible thermomechanical effect.

Figure 5 shows the thermo-electromechanical response under the presence of 1.0 kV/mm electric field at 0.5 °C/min. G′ at 30 °C and 1.0 kV/mm is 3.5×10^5 Pa, which is higher than G′ at 30 °C and 0 kV/mm by about two times. This is due to the BMIM$^+$ and cellulosic hydroxyl group polarizations under an electric field inducing dipole moments and higher G′ [11]. As temperature is increased to 35 °C, G′ approaches its maximum value of 3.6×10^5 Pa, as temperature also promotes these polarizations. Nevertheless, G′ declines as temperature is increased to 60 °C. This is because temperature promotes chloride anion movement towards the anodic electrode under an electric field, producing fewer chloride anion crosslinking species and thus a lower G′ [11, 28, 29]. In the temperature-decreasing step, G′ decreases via the recrystallization of BMIM$^+$Cl$^-$ with a lower rate of G′ depletion compared to that under absence of an electric field. This suggests that an electric field directly affects the recrystallization BMIM$^+$Cl$^-$ at 0.5 °C/min. The electric field induces the ionic polarization of BMIM$^+$Cl$^-$ which produces a smaller BMIM$^+$Cl$^-$ concentration in the middle of the sample, and induces a faster recrystallization at higher temperature. In
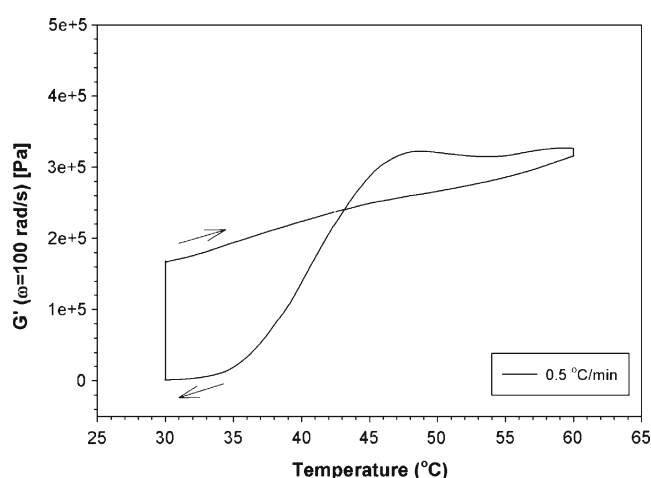
Fig. 4 Shear storage modulus (G′) at 100 rad/s vs. temperature of CelGel at 0.5 °C/min under 0.0 kV/mm
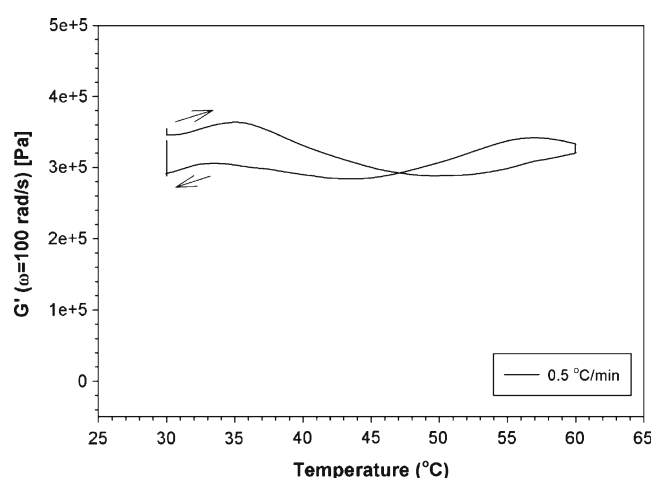
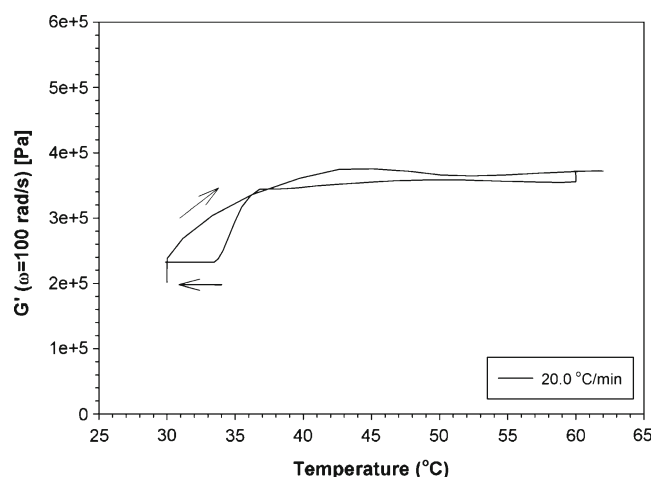**Fig. 5** Shear storage modulus (G′) at 100 rad/s vs. temperature of CelGel at 0.5 °C/min under 1.0 kV/mm

other words, a higher BMIM$^+$Cl$^-$ concentration provides a sluggish recrystallization [17]. In addition, during the holding step at 60 °C and the decreasing step from 60 °C to 47 °C, G′ is higher than that in the increasing step. This results from increases in the cellulosic hydroxyl-chloride anion interaction and the dipole moments generated from the ionic and electronic polarizations under an applied electric field. Between 47 °C to 30 °C, G′ is quite constant at around 3.0×10^5 Pa, then recovers a value close to the initial G′ value in the holding step at 30 °C.

Figure 6 shows the thermo-electromechanical response in the absence of electric field at 20.0 °C/min. In the temperature-increasing step from 30 °C to 60 °C, the data can be divided to two regimes. The first regime is between 30 °C to 53 °C, where G′ abruptly increases from 1.5×10^5 to 6.5×10^5 Pa because the cellulosic hydroxyl-chloride anion interaction, the BMIM$^+$ polarization, the cellulosic hydroxyl polarization, and the cellulose chain expansion [16] are strongly enhanced at the heating rate of 20.0 °C/min. The second regime is between 53 °C to 60 °C; G′ is steady around 6.6×10^5 Pa, which may result from the saturation of those interactions, the polarizations, and the expansion. In the holding step at 60 °C, G′ slightly decreases because of the relaxation of those interactions, the polarizations, and the expansion at the high heating rate. In the temperature-decreasing step from 60 °C to 30 °C, G′ slightly increases to 6.4×10^5 Pa. This results from the cellulose chain entanglement in which it has little time to disentangle until the holding step at 30 °C [16].

Figure 7 shows the thermo-electromechanical response under the presence of 1.0 kV/mm of electric field strength at 20.0 °C/min. G′ data can also be separated into two regimes: temperature-increasing regime (30 °C to 42.5 °C) and the saturating regime (42.5 °C to 60 °C). The increasing temperature regime occurs due to the stronger cellulosic hydroxyl-chloride anion interaction, the BMIM$^+$ polarization, the cellulosic hydroxyl polarization, and the cellulose chain expansion.
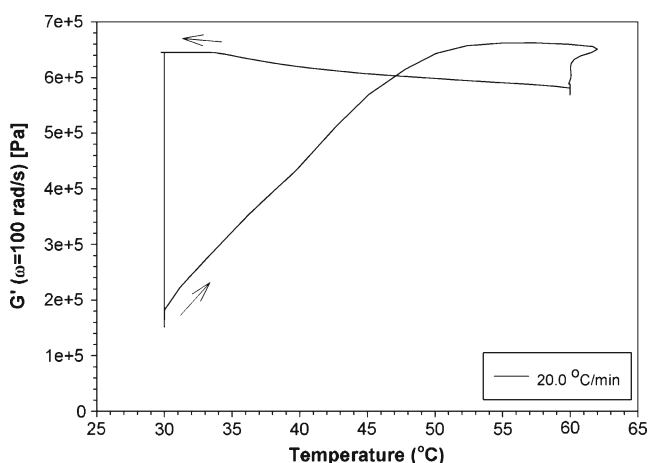
Fig. 7 Shear storage modulus (G′) at 100 rad/s vs. temperature of CelGel at 20.0 °C/min under 1.0 kV/mm

However, the increase in G′ between 30 °C to 43 °C at 20.0 °C/min under 1.0 kV/mm is lesser than that of 0.0 kV/mm. This occurs as the chloride anion leaves out of its crosslinking position to become polarized under 1.0 kV/mm, thus inducing a lower G′. In addition, G′ between 42.5 °C to 60 °C becomes saturated around 3.6×10^5 Pa and stays constant. At the heating rate of 20.0 °C/min, it provides a shorter time scale than that of 0.5 °C/min, so there is less time to allow chloride anions to leave out of the crosslinking position. In the holding step (at 60 °C) and in the decreasing step (60 °C to 37 °C), G′ shows a slightly lower value than that in the increasing step, because these steps provide a period of time for chloride anion movement. G′ decreases when temperature is decreased from 37 °C to 34 °C due to the BMIM$^+$Cl$^-$ crystallization, then becomes saturated and recovers nearly its initial G′. In summary, an electric field causes the ionic polarization of BMIM$^+$Cl$^-$ and a faster recrystallization at higher temperature [17].

Thermal properties under absence of electric field at non-equilibrium

The thermal properties of CelGel, BMIMCl, and cellulose were investigated via DSC as shown in Fig. 8. In the case of 0.5 °C/min, CelGel exhibits an endothermic peak as temperature is increased from 30 °C to 60 °C, which can be related to the melting temperature of BMIM$^+$Cl$^-$ and hydroxyl group rearrangement of cellulose in the CelGel. In addition, CelGel shows an exothermic peak when temperature is decreased from 60 °C to 30 °C, which can be related to the recrystallization of BMIM$^+$Cl$^-$ and hydroxyl group repacking of cellulose in CelGel. When the heating rate is increased to 20.0 °C/min, the melting process of BMIM$^+$Cl$^-$ and hydroxyl group rearrangement of cellulose are promoted in incremental steps, as shown by increasing enthalpy through the integrated

Fig. 6 Shear storage modulus (G′) at 100 rad/s vs. temperature of CelGel at 20.0 °C/min under 0.0 kV/mm

Fig. 8 Differential scanning calorimetric curves and programmed temperature profiles of CelGel, BMIMCl, and cellulose at 0.5 and 20.0 °C/min; A_i=integrated area in temperature increment zone, A_d=integrated area in temperature decrement zone, A_{iso}=integrated area in isothermal zone
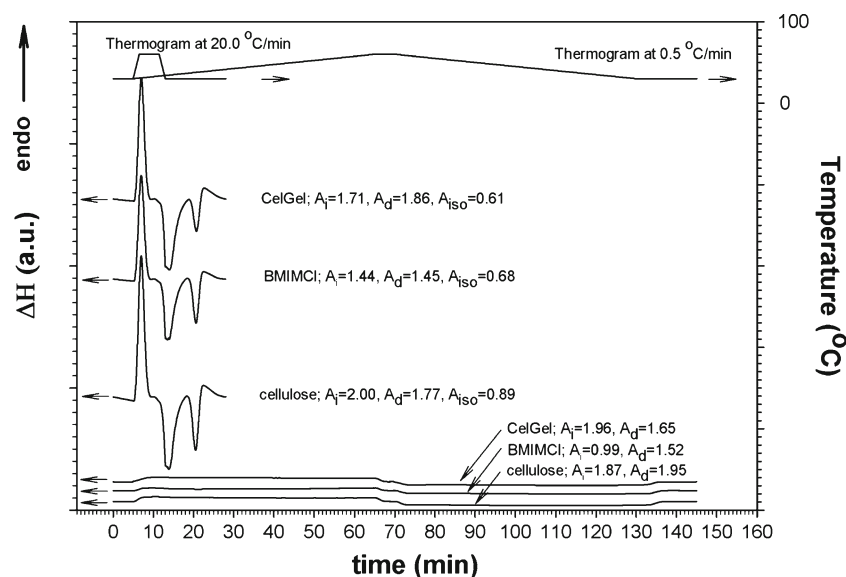
area. However, CelGel shows decreasing enthalpy because its heterogeneity obstructs these processes. In other words, the lower enthalpy of CelGel at 20.0 °C/min compared to 0.5 °C/min is related to a lesser softening process and a more solid-like behavior. This is the cause of dramatically increasing G′ of CelGel in increasing temperature from 30 °C to 60 °C as shown in Fig. 6. In the decreasing step of 20.0 °C/min, the recrystallization of $BMIM^+Cl^-$ and hydroxyl group repacking of cellulose in CelGel are promoted by its heterogeneity [30]. Nevertheless, the recrystallization of $BMIM^+Cl^-$ and hydroxyl group repacking of cellulose are reduced due to a shorter time scale. All of the samples (CelGel, $BMIM^+Cl^-$, and cellulose) showed second exothermic peaks, implying that a longer time for the recrystallization of $BMIM^+Cl^-$, the hydroxyl group repacking, and the relaxation process of cellulose [16] is required in the isothermal region [31]. As shown, both $BMIM^+Cl^-$ and cellulose play important roles in the thermal properties of CelGel in the absence of an electric field in non-equilibrium.

Conclusion

The thermo-electromechanical responses of 1-butyl-3-methylimidazolium chloride ($BMIM^+Cl^-$)-cellulose gel, namely CelGel, were investigated via an oscillatory shear experiment. CelGel was subjected to heat under temperatures between 30 °C to 60 °C under equilibrium and non-equilibrium states, satisfying the conditions of $\tau_m << \tau_e >> \tau_r$ and $\tau_m << \tau_e << \tau_r$, respectively. The electromechanical response in terms of G′ in the equilibrium state is temperature history-independent, with equivalent G′ values in both the increasing and decreasing steps at any temperature. At equilibrium state in the absence of an electric field, G′ increases

with increasing temperature from 30 °C to 50 °C. This results from the stronger interaction of the cellulosic hydroxyl group and the chloride anion, which is confirmed by the decrease in the 3402 cm^{-1} absorbance peak via FTIR investigation. When temperature is increased from 50 °C to 60 °C, G′ decreases because it is close to the melting temperature of $BMIM^+Cl^-$, inducing lower G′. In equilibrium state in the presence of 1 kV/mm of electric field strength, G′ continuously decreases with increasing temperature from 30 °C to 60 °C, as the chloride anion moves out of its crosslinking position to become polarized under an electric field. The electromechanical response in term of G′ in the non-equilibrium state is significantly temperature history-dependent, with different G′ values in the increasing and decreasing steps at certain temperature. The heating rate effect in the absence of an electric field is investigated between 0.5 and 20.0 °C/min. In the increasing step, G′ increases because of the stronger interaction between the cellulosic hydroxyl group and the chloride anion, including a cellulose chain expansion. In the decreasing step, G′ remains constant at higher level because it needs a longer time to relax. These results can be further investigated by DSC curve. The effect of heating rate is investigated at 0.5 and 20.0 °C/min under 1 kV/mm of electric field strength. In the increasing step, G′ increases with a slower rate because of the shorter time scale available for the $BMIM^+$ polarization. In the decreasing step, the recrystallization occurs at lower temperature because a shorter time scale obstructs the recrystallization process. The results suggest that an increase in the heating rate on CelGel retards the melting and promotes recrystallization processes in terms of enthalpy due to its heterogeneity. However, the $BMIM^+Cl^-$ recrystallization and chain relaxation need a longer time, as evidenced by the second DSC peak at 30 °C. The thermo-electromechanical

properties of CelGel have been shown to be drastically different in the equilibrium and non-equilibrium states.

References

1. Klemm D, Heublein B, Fink HP, Bohn A (2005) Cellulose: Fascinating biopolymer and sustainable raw material. Angew Chem Int Ed 44(22):3358–3393
2. Pukada E (2000) History and recent progress in piezoelectric polymers. IEEE Trans Ultrason Ferroelectr Freq Control 47(6):1277–1290
3. Kim J, Yun S, Ounaies Z (2006) Discovery of cellulose as a smart material. Macromolecules 39(12):4202–4206
4. Swatloski RP, Spear SK, Holbrey JD, Rogers RD (2002) Dissolution of cellose with ionic liquids. J Am Chem Soc 124(18):4974–4975
5. Novoselov NP, Sashina ES, Kuz'mina OG, Troshenkova SV (2007) Ionic liquids and their use for the dissolution of natural polymers. Russ J Gen Chem 77(8):1395–1405
6. Lu W, Fadeev AG, Qi B, Smela E, Mattes BR, Ding J, Spinks GM, Mazurkiewicz J, Zhou D, Wallace GG, MacFarlane DR, Forsyth SA, Forsyth M (2002) Use of ionic liquids for π-conjugated polymer electrochemical devices. Science 297(5583):983–987
7. Bennett MD, Leo DJ, Wilkes GL, Beyer FL, Pechar TW (2006) A model of charge transport and electromechanical transduction in ionic liquid-swollen Nafion membranes. Polymer 47(19):6782–6796. doi:10.1016/j.polymer.2006.07.061
8. Bennett MD, Leo DJ (2004) Ionic liquids as stable solvents for ionic polymer transducers. Sensors Actuators A Phys 115(1):79–90. doi:10.1016/j.sna.2004.03.043
9. Ji K, Ma M, Kaneko Y (2008) A facile preparation of gel materials from a solution of cellulose in ionic liquid. Carbohydr Res 343(4):769–772
10. Kunchornsup W, Sirivat A (2010) Effects of crosslinking ratio and aging time on properties of physical and chemical cellulose gels via 1-Butyl-3-methylimidazolium chloride solvent. J Sol-Gel Sci Technol 56(1):19–26
11. Kunchornsup W, Sirivat A (2012) Physically cross-linked cellulosic gel via 1-butyl-3-methylimidazolium chloride ionic liquid and its electromechanical responses. Sensors Actuators A Phys 175(0):155–164. doi:10.1016/j.sna.2011.12.045
12. Pritchard J, Ramesh R, Bowen CR (2004) Time–temperature profiles of multi-layer actuators. Sensors Actuators A Phys 115(1):140–145. doi:10.1016/j.sna.2004.04.019
13. Yoon GH (2012) Topological layout design of electro-fluid-thermal-compliant actuator. Comput Methods Appl Mech Eng 209–212(0):28–44. doi:10.1016/j.cma.2011.11.005
14. Li T, Chen YH, Boey FYC, Ma J (2007) High amplitude vibration of piezoelectric bending actuators. J Electroceram 18(3–4):231–242
15. Putz AMV, Burghelea TI (2009) The solid–fluid transition in a yield stress shear thinning physical gel. Rheol Acta 48(6):673–689
16. Ruan D, Lue A, Zhang L (2008) Gelation behaviors of cellulose solution dissolved in aqueous NaOH/thiourea at low temperature. Polymer 49(4):1027–1036. doi:10.1016/j.polymer.2007.12.044
17. Akbulut O, Taniguchi I, Kumar S, Shao-Horn Y, Mayes AM (2007) Conductivity hysteresis in polymer electrolytes incorporating poly(tetrahydrofuran). Electrochim Acta 52(5):1983–1989. doi:10.1016/j.electacta.2006.08.007
18. Tungkavet T, Sirivat A, Seetapan N, Pattavarakorn D (2013) Stress relaxation behavior of (Ala-Gly-Pro-Arg-Gly-Glu-4Hyp-Gly-Pro-) gelatin hydrogels under electric field: Time-electric field superposition. Polymer (United Kingdom) 54(9):2414–2421
19. Gonjo T, Futami Y, Morisawa Y, Wojcik MJ, Ozaki Y (2011) Hydrogen bonding effects on the wavenumbers and absorption intensities of the OH fundamental and the first, second, and third overtones of phenol and 2,6-dihalogenated phenols studied by visible/near-infrared/infrared spectroscopy. J Phys Chem A 115(35):9845–9853
20. Domańska U, Bogel-Łukasik E (2004) Solid–liquid equilibria for systems containing 1-butyl-3-methylimidazolium chloride. Fluid Phase Equilib 218(1):123–129
21. Iotti M, Gregersen ØW, Moe S, Lenes M (2011) Rheological Studies of Microfibrillar Cellulose Water Dispersions. J Polym Environ 19(1):137–145
22. Nelson ML, O'Connor RT (1964) Relation of certain infrared bands to cellulose crystallinity and crystal lattice type. Part II. A new infrared ratio for estimation of crystallinity in celluloses I and II. J Appl Polym Sci 8(3):1325–1341. doi:10.1002/app.1964.070080323
23. Zhbankov RG, Firsov SP, Korolik EV, Petrov PT, Lapkovski MP, Tsarenkov VM, Marchewka MK, Ratajczak H (2000) Vibrational spectra and the structure of medical biopolymers. J Mol Struct 555:85–96
24. Langkilde FW, Svantesson A (1995) Identification of celluloses with Fourier-transform (FT) mid-infrared, FT-Raman and near-infrared spectrometry. J Pharm Biomed Anal 13(4–5):409–414
25. Spiridon I (2007) Modifications of Asclepias syriaca fibers for paper production. Ind Crop Prod 26(3):265–269. doi:10.1016/j.indcrop.2007.03.015
26. Seo J, Kim J, Koh J, Ahn S, Kim J (2009) Preparation and characterization of crosslinked cellulose/sulfosuccinic acid membranes as proton conducting electrolytes. Ionics 15(5):555–560. doi:10.1007/s11581-009-0314-8
27. Chang HC, Jiang JC, Chang CY, Su JC, Hung CH, Liou YC, Lin SH (2008) Structural organization in aqueous solutions of 1-butyl-3-methylimidazolium halides: A high-pressure infrared spectroscopic study on ionic liquids. J Phys Chem B 112(14):4351–4356
28. Mahadeva SK, Kim J (2009) Electromechanical behavior of room temperature ionic liquid dispersed cellulose. J Phys Chem C 113(28):12523–12529
29. Mahadeva SK, Yi C, Kim J (2009) Effect of room temperature ionic liquids adsorption on electromechanical behavior of cellulose electroactive paper. Macromol Res 17(2):116–120
30. König A, Stepanski M, Kuszlik A, Keil P, Weller C (2008) Ultra-purification of ionic liquids by melt crystallization. Chem Eng Res Des 86(7):775–780. doi:10.1016/j.cherd.2008.04.002
31. Calvar N, Gómez E, Macedo EA, Domínguez A (2013) Thermal analysis and heat capacities of pyridinium and imidazolium ionic liquids. Thermochim Acta 565(0):178–182. doi:10.1016/j.tca.2013.05.007